Pergamon

Bioorganic & Medicinal Chemistry 8 (2000) 751–768

BIOORGANIC & MEDICINAL CHEMISTRY

Synthesis, Antiplatelet Activity and Comparative Molecular Field Analysis of Substituted 2-Amino-4*H*-pyrido[1,2-*a*]pyrimidin-4-ones, their Congeners and Isosteric Analogues

Giorgio Roma,[a,*] Nunzia Cinone,[c] Mario Di Braccio,[a] Giancarlo Grossi,[a] Giuliana Leoncini,[b] Maria Grazia Signorello[b] and Angelo Carotti[c,*]

[a]*Dipartimento di Scienze Farmaceutiche, Università di Genova, viale Benedetto XV, 16132 Genoa, Italy*
[b]*Dipartimento di Medicina Sperimentale, Sezione Biochimica, Università di Genova, viale Benedetto XV, 16132 Genoa, Italy*
[c]*Dipartimento Farmacochimico, Università di Bari, via Orabona 4, 70125 Bari, Italy*

Received 27 May 1999; accepted 19 October 1999

Abstract—2-(1-Piperazinyl)-4*H*-pyrido[1,2-*a*]pyrimidin-4-one (**5a**) is a recently described in vitro inhibitor of human platelet aggregation which specifically inhibits the activity of high affinity cAMP phosphodiesterase. A number of substitution derivatives, isosteres, and analogues of **5a** were now synthesized and tested in vitro for their inhibitory activity on human platelet aggregation induced in platelet-rich plasma by ADP, collagen, or the Ca^{2+} ionophore A23187. Among the most effective compounds, the 6-methyl, 8-methyl and 6,8-dimethyl derivatives of **5a** resulted nearly as active as the lead when platelet aggregation was induced by ADP or A23187, but less active when collagen was the inducer. On the basis of present results and those previously obtained by us in this and 2-aminochromone structural fields, we have developed a statistically significant 3-D QSAR model, using comparative molecular field analysis (CoMFA), describing the variation of the antiplatelet activity in terms of molecular steric and electrostatic potential changes.

Introduction

In the course of our previous chemical and pharmacological studies on 2-(dialkylamino)chromones **1** and their benzo-fused derivatives **2**, **3** and **4** (Chart 1), whose first examples were described by us,[1–6] we reported the in vitro antiplatelet activity of some 7-substituted compounds **1**.[7–10]

Considering that the platelet aggregation inhibitory properties of some pyrido[1,2-*a*]pyrimidine derivatives had also been reported,[11] we have more recently synthesized and tested for their in vitro antiplatelet activity a number of *N*-substituted 2-amino-4*H*-pyrido[1,2-*a*]-pyrimidin-4-ones **5** ($R^2 = R^3 = H$, $X = O$),[12,13] structurally analogous to compounds **1**, and of their angular benzo-fused derivatives **6** and **7**,[13] as well as some examples of compounds **8**, **9** and **10**,[13] isomers of **5** ($R^2 = R^3 = H$, $X = O$), **6** and **7**, respectively (Chart 2).

The interesting platelet anti-aggregating properties shown in vitro by some of the 1,2-fused pyrimidine derivatives **5**–**10**[13] subsequently prompted us to widen the study also in the field of fused pyran derivatives. Thus, we synthesized a group of properly chosen compounds **1**–**3** and **11**–**13** (Chart 3), structural analogues of compounds **5**–**7** and **8**–**10**, respectively, and evaluated their in vitro antiplatelet activity. Also some of the compounds **1**–**3**, **11**–**13** were significantly active.[14]

On the whole, if we consider the antiplatelet activity data obtained in the above studies for all classes of compounds tested (**1**–**3**, **5**–**13**) towards all the platelet aggregation inducers used (i.e. adenosine diphosphate (ADP), collagen, and the Ca^{2+} ionophore A23187 (calcimycin)), the following remarks can be made.

- 1-Piperazinyl proved to be the most effective amino substituent among all those used. Actually the (1-piperazinyl) substituted compound (N(R, R1) = N NH) was the most active one in each structural class, generally towards all platelet aggregation inducers (in the case of compounds **8**–**10** this derivative was not obtainable).

*Corresponding authors. AC. Tel.: +39-080-5442782; fax: +39-080-5442230; e-mail: carotti@farmchim.uniba.it GR. Tel.: +31-010-3538374; fax: +39-010-3538358.

0968-0896/00/$ - see front matter
PII: S0968-0896(00)00010-9

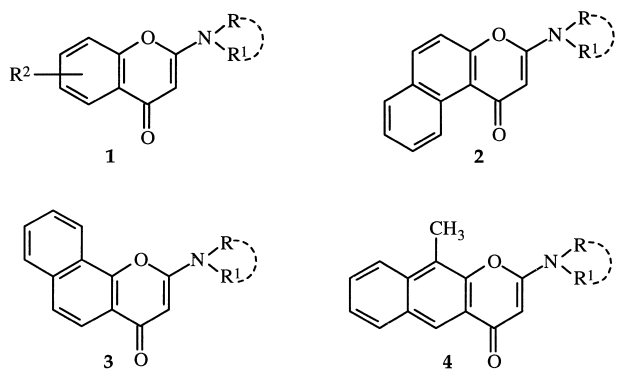

Chart 1.

- The (1-piperazinyl) substituted compounds **5–7** were more active than the corresponding compounds **1–3**.
- The activities of (1-piperazinyl) substituted coumarin derivatives **11–13** were very similar to those of the corresponding chromone derivatives **1–3**.
- The 2-(1-piperazinyl) substituted compound **5a** was the most active of all compounds tested, whereas 7-ethoxy-4-(1-piperazinyl)coumarin **11b** was the most active of the fused pyran derivatives **1–3**, **11–13** (Table 1).

For convenience, the IC_{50} values of the most active of all the compounds tested in the above studies[7–10,12–14] are summarized in Table 1.

In the light of these results, we can plainly conclude that 2-(1-piperazinyl)-4*H*-pyrido[1,2-*a*]pyrimidin-4-one (**5a**) is the most interesting in vitro inhibitor of human platelet aggregation among compounds **1–3**, **5–13** previously prepared and tested by us,[7–10,12–14] with respect both to the heterocyclic nucleus and the dialkylamino substituent.

For this reason we have now been dealing with the synthesis and biological evaluation of several new compounds (**5b–r**, **17a,b**, **19a–d** and **20**), whose structures have been derived from that of **5a** through proper modifications of the pyridine ring and/or the 2-substituent, aiming at reaching higher antiplatelet activities and widening the knowledge of structure–activity relationships in this field. The chemical and biological results of this study are reported in this paper.

Furthermore, an extended antiplatelet activity data set, obtained by adding the actual results to those previously reported for compounds **1–3**, **11–13**[14] and **5–10**[12,13] has been submitted to a 3-D QSAR (CoMFA) study which is also described here.

The platelet antiaggregating properties of compound **5a** derive from its ability to specifically inhibit the activity of high affinity cAMP phosphodiesterase and, consequently, increase intracellular cAMP concentration.[15]

Chemistry

Syntheses of intermediates **14a–c**, **15b,c,i,j** and **18a**, and of final compounds **5b–r**, **17a,b**, **19a–d** and **20** are depicted in Schemes 1 and 2, respectively.

According to a synthetic route previously reported in the literature,[16] the reaction at room temperature of the suitable acyl chlorides with heteroarylamines afforded the *N*-substituted ethyl malonamates **14a–c** that were in turn heated with a mixture of polyphosphoric acid and phosphorus oxychloride to give the chloroderivatives

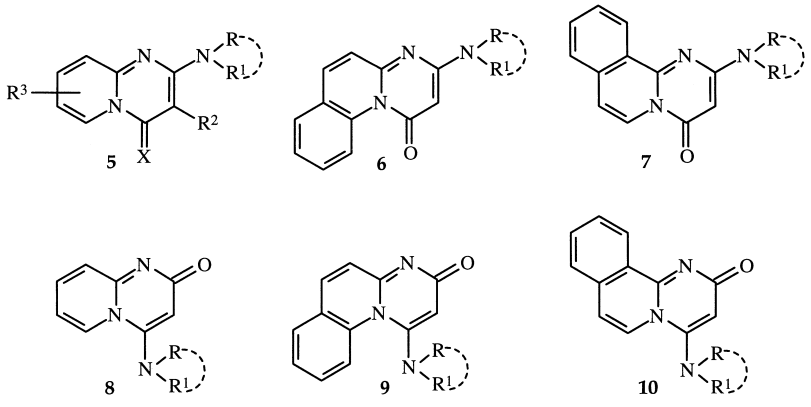

Chart 2.

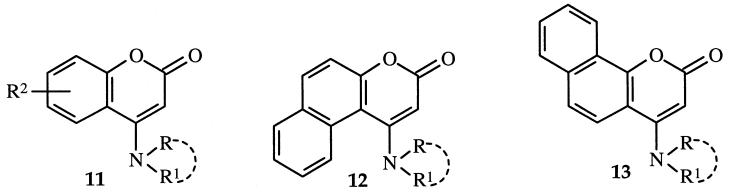

Chart 3.

Table 1. In vitro inhibitory activity of (1-piperazinyl) substituted compounds **1–3**, **5–7**, **11–13** (Charts 1–3) on human platelet aggregation induced in PRP[a] by ADP, collagen and A23187

Compound[b]		R^2	R^3	X	IC_{50} (μM) ± SD		
					ADP (5.0 μM)	Collagen (10.0 μg/mL)[c]	A23187 (20.0 μM)
1a		H	—	—	56 ± 13	60 ± 12	240 ± 90
2a		—	—	—	39 ± 3	56 ± 16	201 ± 61
3a		—	—	—	119 ± 40	117 ± 32	278 ± 15
5a		H	H	O	6 ± 1.8	3.6 ± 1.2	19 ± 9
6a		—	—	—	13 ± 4	15 ± 8	28 ± 8
7a		—	—	—	38 ± 10	21 ± 9	54 ± 17
11a		H	—	—	49 ± 14	36 ± 10	250 ± 38
11b		7-OC_2H_5	—	—	24 ± 14	10 ± 3.6	44 ± 18
12a		—	—	—	53 ± 15	49 ± 17	245 ± 65
13a		—	—	—	81 ± 23	71 ± 27	334 ± 89

[a]PRP = platelet-rich plasma.
[b]Compounds **5a**, **6a**, **7a**: ref 13; compounds **1a**, **2a**, **3a**, **11a,b**, **12a**, **13a**: ref 14.
[c]5.0 μg/mL for compounds **5a**, **6a**, **7a**.

15b,i and **18a**, respectively. On the other hand, the chloroderivatives **15c,j** were prepared through the reaction of 2-chloro-4*H*-pyrido[1,2-*a*]pyrimidin-4-one (**15a**)[17] with bromine at room temperature or the Lawesson's reagent in refluxing toluene, respectively.

The substituted 2-amino-4*H*-pyrido[1,2-*a*]pyrimidin-4-ones **5c–j,l–r** and 4-thione analogue **5k** (see Table 2) were generally obtained in high yields by treating the corresponding 2-chloroderivatives **15a–j** with excess amines (ethanol at reflux), whereas 3-nitro-2-(1-piperazinyl)-4*H*-pyrido[1,2-*a*]pyrimidin-4-one (**5b**) (Table 2) was prepared through the nitration of compound **5a**[13] with a mixture of concentrated nitric and sulfuric acids.

By heating a solution of 2-chloroderivative **15a** in ethylene glycol, in the presence of anhydrous potassium carbonate, 2-(2-hydroxyethoxy)-4*H*-pyrido[1,2-*a*]pyrimidin-4-one (**17b**) was obtained. The treatment of 7-chloroderivatives **18b**[18] or **18c**[19] with excess piperazine (refluxing ethanol) gave high yields of 7-(1-piperazinyl)-5*H*-thiazolo[3,2-*a*]pyrimidin-5-one (**19b**) or its 2,3-dihydroderivative **19d**, respectively. The same treatment of 5-chloroderivative **18a** afforded a lower yield of 2-methyl-5-(1-piperazinyl)-7*H*-isoxazolo[2,3-*a*]pyrimidin-7-one (**19a**). Moreover, also (chloromethyl)derivatives **16a,b**[20] reacted with piperazine under similar conditions to give the [(1-piperazinyl)methyl] derivatives **17a** and **20**, respectively. Finally, the hydrogenation of compound **5a,** using 5% palladium on activated charcoal as catalyst, afforded the tetrahydroderivative **19c**.

The structures attributed to the compounds described in this paper are supported by the results of elemental analyses and IR and ^{1}H NMR spectral data (see Experimental and Table 3).

Thus, β-enaminonic compounds **5b–j,l–r** afforded characteristic ^{1}H NMR signals for protons H-3 (singlet) and H-6 at δ 5.27–5.67 and 8.71–8.99, respectively, and the ν CO IR band at 1656–1680 cm^{-1}, as we previously observed in this structural field.[12,13,21–24] Only the ^{1}H NMR H-3 singlet of **5p** is shifted more downfield (δ 6.11), due to the lower shielding effect of 2-hydrazino substituent on this proton.[12]

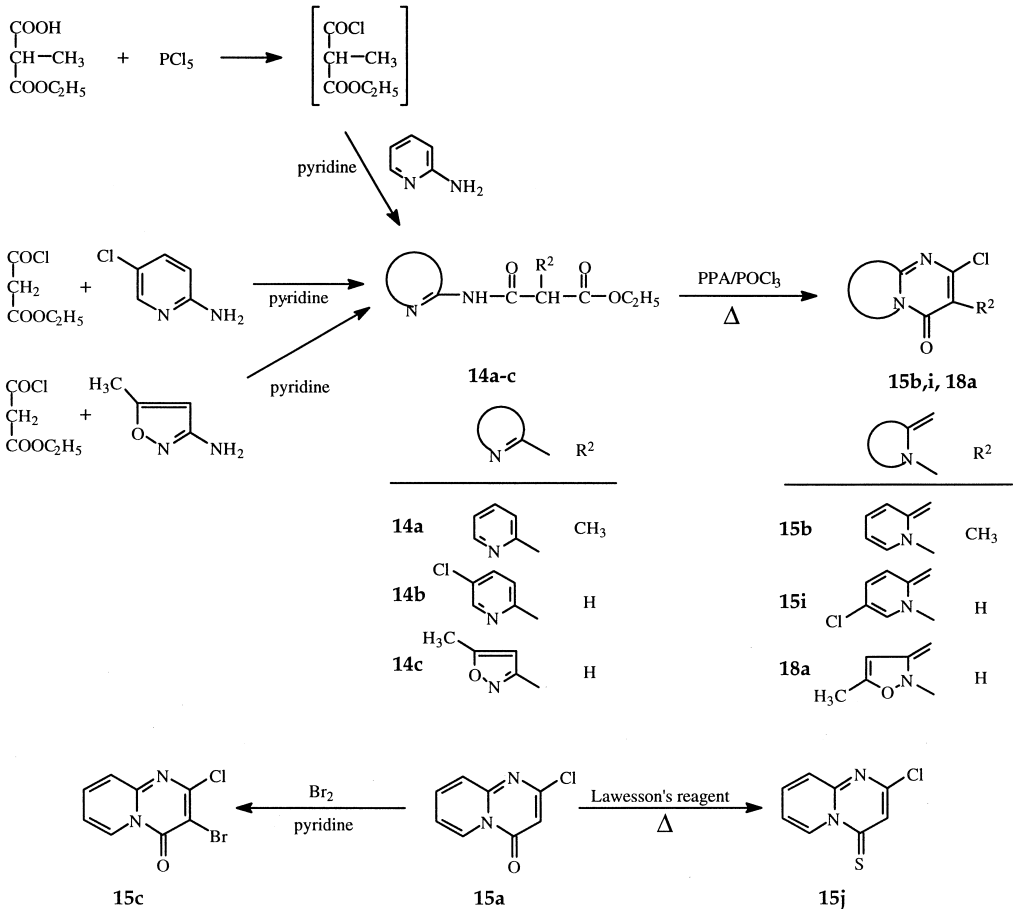

Scheme 1.

Also the spectra of compounds **19a–d** show the ^{1}H NMR singlet of the pyrimidine hydrogen at δ 5.17–5.39 and the ν CO IR band at 1640–1663 cm^{-1}, in accordance with the above results and their structural similarity with compounds **5** (X = O, R^2 = H).

Finally, it is interesting to remark that the replacement of the (1-piperazinyl) substituent of compounds **5a**[13] and **19b** with a [(1-piperazinyl)methyl] group (compounds **17a** and **20**, respectively) resulted in a decreased shielding of the pyrimidine hydrogen of latter compounds and in the consequent appreciable downfield shift of its ^{1}H NMR signal ($CDCl_3$), due to the lack of the enamino substituent and of its electron-releasing resonance effect.

Results and Discussion

Structure–activity relationships (SAR)

Compounds **5b–r**, **17a,b**, **19a–d** and **20** were tested in vitro for their inhibitory activity on the aggregation of human platelets induced in platelet-rich plasma (PRP) by adenosine diphosphate (ADP), collagen, or the Ca^{2+} ionophore A23187 (calcimycin) (see Experimental). Acetyl salicylic acid (ASA), trifluoperazine, and propranolol were also tested under the same conditions as reference compounds. The IC_{50} values obtained are reported in Table 2 and suggest the following remarks with reference to the three groups below of compounds, which are structurally related to **5a**, taken as a lead (see Table 1).

Compounds 5l–r, 17a,b (deriving from modification of 1-piperazinyl substituent of 5a) and 20

The activities of these compounds are far lower than that of **5a**. In particular, these results seem to indicate that the open chain 2-substituents (**5q,r**, **17b**), the steric hindrance at 1-piperazinyl NH group (**5l**), as well as the lack of the direct link of 1-piperazinyl group to position 2 (**17a**, **20**) are structural features unfavorable to antiplatelet activity of these analogues of **5a**. Even the 1-homopiperazinyl substituent (**5m**) is far less effective than 1-piperazinyl.

Compounds 19a–d (deriving from modification of pyridine ring of 5a)

When ADP or A23187 were used as platelet aggregation inducers, isoxazolo[2,3-*a*]pyrimidine and thiazolo[3,2-*a*]-pyrimidine derivatives **19a** and **19b**, respectively, resulted in being moderately less effective than their isosteric

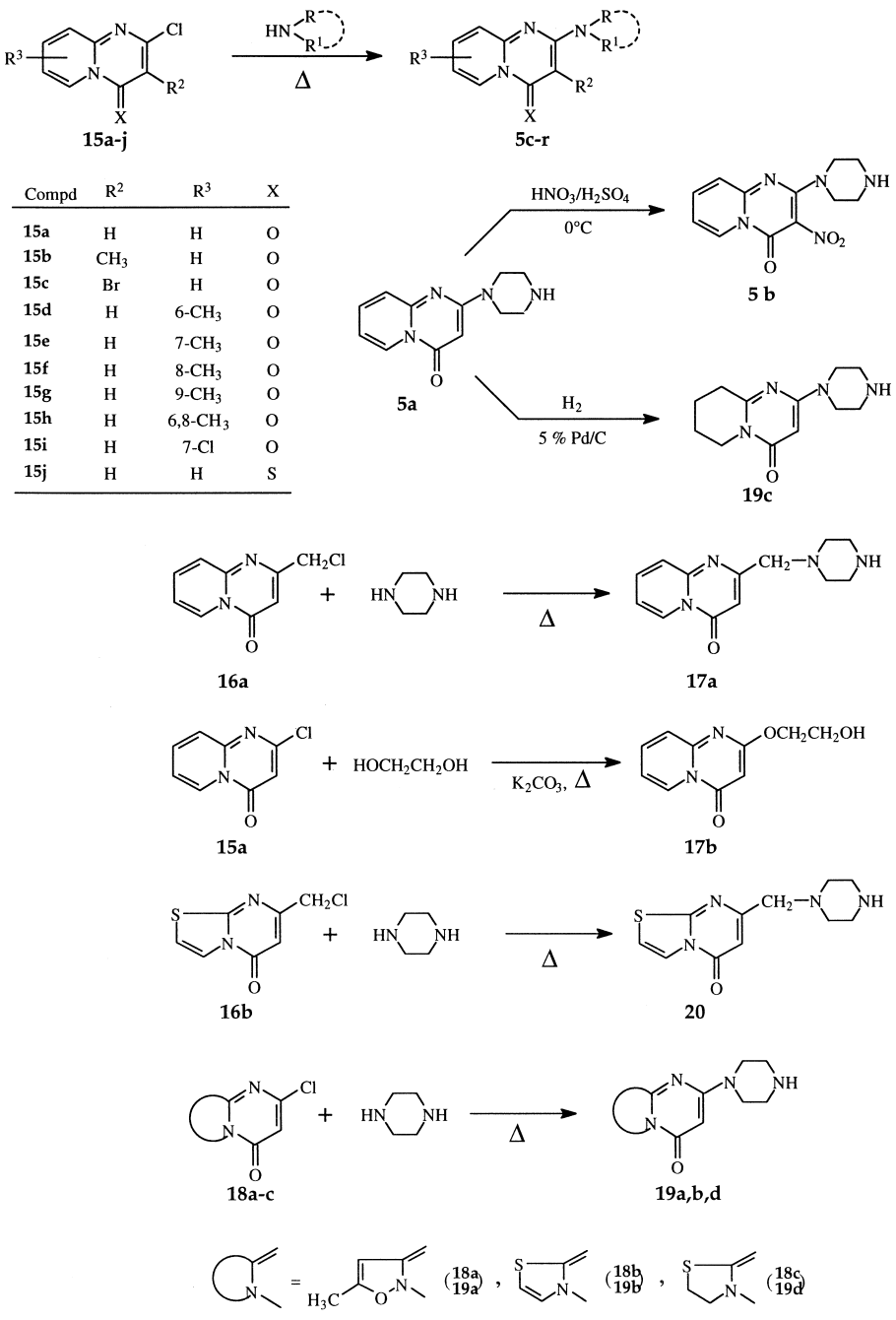

Scheme 2.

analogue **5a**, as well as the hydrogenated derivatives **19c** and **19d** compared with their respective parent compounds **5a** and **19b**. When collagen was used, the difference of activity between compounds **19a**, **19b** or **19c** and compound **5a** proved to be rather higher.

Compounds 5b–j (deriving from introduction of further substituents into 5a nucleus) and 5k

All the compounds of this group are less active than the parent, except for methylderivatives **5e–g,i** and chloroderivative **5j** which are nearly equiactive to **5a** towards ADP and A23187. The presence of substituents in positions 3 and 9 of the 4*H*-pyrido[1,2-*a*]pyrimidine nucleus appears especially unfavorable (compare the IC_{50} values of methylderivatives **5c,h** with those of **5e–g,i**). Moreover, the introduction of electron withdrawing 3-substituents into **5a** affords derivatives (**5b,d**) considerably less active than the parent compound.

Three dimensional quantitative structure–activity relationships (3-D QSAR)

The in vitro antiplatelet activity data reported in Tables 4–9 were subjected to a 3-D QSAR study by means of Comparative Molecular Field Analysis (CoMFA).[25]

Table 2. In vitro inhibitory activity of compounds **5b–r**, **17a,b**, **19a–d, 20** on platelet aggregation induced in human PRP by ADP, collagen and A23187

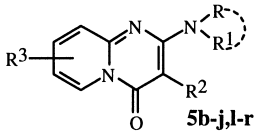
5b-j,l-r

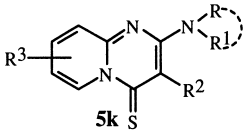
5k

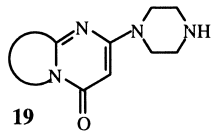
19

Compound[a]		R^2	R^3	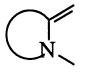	IC_{50} (μM) ± SD		
					ADP (5.0 μM)	Collagen (5.0 μg/mL)	A23187 (20.0 μM)
5b		NO_2	H	—	366 ± 108	789 ± 90	853 ± 38
5c		CH_3	H	—	28 ± 5	93 ± 26	76 ± 2
5d		Br	H	—	182 ± 38	230 ± 74	202 ± 90
5e		H	6-CH_3	—	5.6 ± 1.7	18.5 ± 3.6	17.4 ± 1
5f		H	7-CH_3	—	8.7 ± 1.2	18.5 ± 5.6	15.5 ± 5.8
5g		H	8-CH_3	—	5.8 ± 0.7	16.2 ± 3.8	15.8 ± 6.4
5h		H	9-CH_3	—	76.5 ± 2.8	93.5 ± 44.6	177 ± 17
5i		H	6,8-CH_3	—	5.1 ± 1.0	14.6 ± 3.3	19.6 ± 7.6
5j		H	7-Cl	—	9.9 ± 2.7	20.7 ± 5.3	17.8 ± 5.9
5k		H	H	—	75 ± 8	160 ± 32	142 ± 34
5l	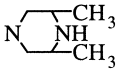	H	H	—	970 ± 45	>1000	>1000
5m		H	H	—	270 ± 39	564 ± 83	777 ± 156
5n	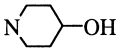	H	H	—	>1000	>1000	>1000
5o	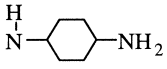	H	H	—	958 ± 59	891 ± 13	731 ± 185
5p		H	H	—	>1000	>1000	>1000
5q	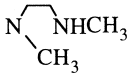	H	H	—	>1000	>1000	>1000
5r	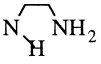	H	H	—	>1000	>1000	>1000
19a	—	—	—	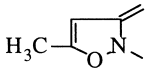	15.6 ± 3.2	39.4 ± 10	49.0 ± 15
19b	—	—	—		19.5 ± 4.5	46.4 ± 3.3	51.3 ± 10
19c	—	—	—		27 ± 4	97.4 ± 13	53 ± 9
19d	—	—	—		130 ± 20	197 ± 41	265 ± 77
ASA					>1000	159 ± 24	> 1000
Trifluoperazine					180 ± 48	138 ± 41	318 ± 61
Propranolol					291 ± 76	131 ± 31	269 ± 62

[a]The IC_{50} values of compounds **17a,b** and **20** (see Scheme 2) were >1000 μM towards all the three platelet aggregation inducers.

Table 3. Spectral, physicochemical and reaction data of substituted 2-amino-4*H*-pyrido[1,2-*a*]pyrimidin-4-ones **5c–j, l–r** and 2-(1-piperazinyl)-4*H*-pyrido[1,2-*a*]pyrimidine-4-thione **5k**

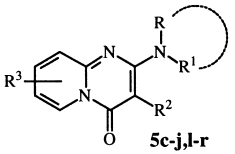

5c-j,l-r

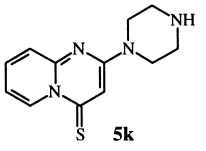

5k

Compound[a]	Reaction time (h)	Yield (%)	mp °C (solv.)[b]	Molecular formula[c]	IR[d] (cm^{-1})	^1H NMR[e] (δ, ppm)
5c	3	82	146–147 (A)	$C_{13}H_{16}N_4O$	3205 (NH), 1658 (CO), 1628, 1552, 1527	1.77[f] (s, 1H, NH), 2.21(s, 3H, CH_3), 3.03 (m, 4H, CH_2NH), 3.47 (m, 4H, NCH_2), 6.98 (m, 1H, H-7), 7.23–7.84 (m, 2H, H-8, 9), 8.98 (m, 1H, H-6)
5d	1	86	150–151 (B)	$C_{12}H_{13}BrN_4O$	3290 (NH), 1666 (CO), 1627, 1552, 1528s	1.74[f] (s, 1H, NH), 3.02 (m, 4H, CH_2NH), 3.75 (m, 4H, NCH_2), 7.02 (m, 1H, H-7), 7.41 (m, 1H, H-9), 7.71 (m, 1H, H-8), 8.99 (m, 1H, H-6)
5e	1	82	140–141 (A)	$C_{13}H_{16}N_4O$	3270 (NH), 1656 (CO), 1638sh, 1554br, 1500	1.90[f] (s, 1H, NH), 2.94 (m, 4H, CH_2NH), 3.01 (s, 3H, CH_3), 3.64 (m, 4H, NCH_2), 5.46 (s, 1H, H-3), 6.46 (dd, 1H, H-7), 7.17 (dd, 1H, H-9), 7.39 (dd, 1H, H-8)
5f	1	62	148–149 (A)	$C_{13}H_{16}N_4O$	3320 (NH), 1663 (CO), 1638, 1540sh, 1530, 1505	2.00[f] (s, 1H, NH), 2.34 (s, 3H, CH_3), 2.94 (m, 4H, CH_2NH), 3.66 (m, 4H, NCH_2), 5.64 (s, 1H, H-3), 7.19 (near d, 1H, H-9), 7.48 (near d, 1H, H-8), 8.71 (near s, 1H, H-6)
5g	1	76	143–144 (A)	$C_{13}H_{16}N_4O$	3290w[g] (NH), 1663 (CO), 1646, 1540sh, 1530, 1500	1.88[f] (s, 1H, NH), 2.37(s, 3H, CH_3), 2.92 (m, 4H, CH_2NH), 3.66 (m, 4H, NCH_2), 5.58 (s, 1H, H-3), 6.70 (near d, 1H, H-7), 7.07 (near s, 1H, H-9), 8.79 (near d, 1H, H-6)
5h	1	70	169–170 (A)	$C_{13}H_{16}N_4O$	3295w[g] (NH), 1660 (CO), 1635, 1540, 1520sh, 1493w	1.87[f] (s, 1H, NH), 2.45 (s, 3H, CH_3), 2.96 (m, 4H, CH_2NH), 3.70 (m, 4H, NCH_2), 5.66 (s, 1H, H-3), 6.79 (dd, 1H, H-7), 7.43 (dd, 1H, H-8), 8.85 (dd, 1H, H-6)
5i	1	74	174–174.5 (A)	$C_{14}H_{18}N_4O$	3305 (NH), 1666 (CO) and 1650 (fused), 1550br, 1500	1.80[f] (s, 1H, NH), 2.24 (s, 3H, 8-CH_3), 2.90 (m, 4H, CH_2NH), 2.96 (s, 3H, 6-CH_3), 3.60 (m, 4H, NCH_2), 5.39 (s, 1H, H-3), 6.29 (near s, 1H, H-7), 6.89 (near s, 1H, H-9)
5j	1	85	191–192 (A)	$C_{12}H_{13}ClN_4O$	3312 (NH), 1670 (CO), 1624, 1550, 1532, 1508	1.85[f] (s, 1H, NH), 2.94 (m, 4H, CH_2NH), 3.67 (m, 4H, NCH_2), 5.61 (s, 1H, H-3), 7.22 (near d, 1H, H-9), 7.54 (dd, $J_{8,9}=9.6$ Hz, $J_{8,6}=2.5$ Hz, 1H, H-8), 8.93 (near d, 1H, H-6)
5k	0.5	92	136–137 (A)	$C_{12}H_{14}N_4S$	3245 (NH), 1640, 1580sh, 1568s, 1548, 1530sh, 1112 (CS)	1.90[f] (s, 1H, NH), 2.95(m, 4H, CH_2NH), 3.77(m, 4H, NCH_2), 6.62–7.99 (m, 3H, H-7, 8, 9), 7.22 (s, 1H, H-3), 10.26 (m, 1H, H-6)
5l	1	90	163–164 (A)	$C_{14}H_{18}N_4O$	3255w (NH), 1672s (CO), 1628, 1556, 1534, 1505br	1.14 (d, 6H, CH_3), 1.66[f] (s, 1H, NH), 2.48 (dd, 2H, axial NCH), 2.77–2.97 (m, 2H, $CHCH_3$), 4.31 (dd, 2H, equatorial NCH), 5.63 (s, 1H, H-3), 6.85 (m, 1H, H-7), 7.27 (m, 1H, H-9), 7.57 (m, 1H, H-8), 8.87 (m, 1H, H-6)
5m	4	74	178–179 (C)	$C_{13}H_{16}N_4O\cdot C_4H_4O_4\cdot 0.5H_2O$	3310[g] (NH), 1660 (CO), 1631, 1554, 1535, 1510sh	1.61–2.12 (m, 2H, CH_2), 2.21[f] (s, 1H, NH), 2.66–3.23 (m, 4H, 2 CH_2NH), 3.53–4.01 (m, 4H, 2 NCH_2), 5.58 (s, 1H, H-3), 6.87 (m, 1H, H-7), 7.27 (m, 1H, H-9), 7.59 (m, 1H, H-8), 8.91 (m, 1H, H-6)
5n	2	96	160–161 (A)	$C_{13}H_{15}N_3O_2$	3595w and 3355br (OH), 1658 (CO), 1631, 1554sh, 1533, 1506sh	1.47–1.67 (m, 2H, β-CH_2), 1.85–2.05 (m, 3H, β-CH_2 + OH; m, 2H, after treatment with D_2O), 3.32 (m, 2H, NCH_2), 3.98 (m, 1H, $CHOH$), 4.06–4.22 (m, 2H, NCH_2), 5.67 (s, 1H, H-3), 6.85 (m, 1H, H-7), 7.28 (m, 1H, H-9), 7.57 (m, 1H, H-8), 8.87 (m, 1H, H-6)
5o	2	87	200–201.5 (D)	$C_{14}H_{18}N_4O$	3345, 3260 w and 3170br (NH + NH_2), 1664 (CO), 1640, 1630sh, 1558br, 1538, 1485	1.04–1.38 (m, 4H, 2 CH_2), 1.70–1.98 (m, 5H, CH NH_2 + 2CH_2), 2.51 (m, 1H, NHCH), 3.30[f] (broad, 2H, NH_2), 5.27 (s, 1H, H-3), 7.00 (m, 1H, H-7), 7.08[f] (d, 1H, NH), 7.26 (m, 1H, H-9), 7.75 (m, 1H, H-8), 8.75 (m, 1H, H-6)
5p	3	30	149–150 (E)	$C_{13}H_{16}N_4O$	3305w (NH), 1668 (CO), 1632, 1577, 1542, 1480	1.00–1.95 (m, 6H, β-CH_2 + γ-CH_2), 2.38–2.98 (m, 4H, NCH_2), 5.73[f] (broad s, 1H, NH), 6.11 (s, 1H, H-3), 6.89 (m, 1H, H-7), 7.23 (m, 1H, H-9), 7.62 (m, 1H, H-8), 8.96 (m, 1H, H-6)
5q	2	60	158–159 (F)	$C_{12}H_{16}N_4O\cdot C_4H_4O_4$	3335w (NH), 1665 (CO), 1637, 1561, 1542, 1511w	1.98[f] (s, 1H, NH), 2.48 (s, 3H, NHCH_3), 2.85 (t, 2H, CH_2NHCH_3), 3.08 (s, 3H, CH_3), 3.76 (t, 2H, NCH_2), 5.53 (s, 1H, H-3), 6.82 (m, 1H, H-7), 7.27 (m, 1H, H-9), 7.54 (m, 1H, H-8), 8.86 (m, 1H, H-6)
5r	2	46	166.5–167 (F)	$C_{10}H_{12}N_4O\cdot C_4H_4O_4$	3460-3210br (NH + NH_2), 1674 (CO), 1642, 1575, 1545, 1480	1.40[f] (s, 2H, NH_2), 2.87 (near t, 2H, CH_2NH_2), 3.27 (m, 2H, NHCH_2), 5.31[f] (broad s, 1H, NH), 5.41 (s, 1H, H-3), 6.79 (m, 1H, H-7), 7.17 (m, 1H, H-9), 7.51 (m, 1H, H-8), 8.83 (m, 1H, H-6)

[a]For compounds **5m**,**q**,**r**, yields, melting points (mp), crystallization solvents, molecular formulas and analyses refer to the corresponding maleates, whereas IR and ^1H NMR spectral data of the free bases are reported.
[b]Crystallization solvents: A = ethyl acetate, B = ethyl acetate/petroleum ether, C = methanol/petroleum ether, D = chloroform, E = isopropyl ether, F = dichloromethane/petroleum ether.
[c]Analyses: C, H, N, Br for **5d**, C, H, N, Cl for **5j**, C, H, N, S for **5k**, C, H, N for all other compounds.
[d]In $CHCl_3$ solution: compounds **5g**,**h**,**m**,**n**,**p**,**q**,**r**; in KBr pellet: compounds **5c**,**d**,**e**,**f**,**i**,**j**,**k**,**l**,**o**.
[e]Solvents: $CDCl_3$ for all compounds except **5o**, for which $(CD_3)_2SO$ was used.
[f]Disappeared with D_2O.
[g]From the spectrum of compound in the solid state (KBr).

Table 4. Chemical structures and platelet antiaggregating activity of compounds of class A

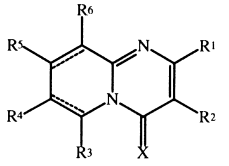

$\mathbf{A_1}$-$\mathbf{A_{50}}$, $\mathbf{A_{52}}$-$\mathbf{A_{59}}$: X=O; $\mathbf{A_{51}}$: X=S.

Compound	R^1	R^2	R^3, R^4	R^5, R^6	pIC_{50}[a]	Ref
$\mathbf{A_1}$	$N(CH_3)_2$	H	H, H	H, H	3.13	12
$\mathbf{A_2}$	$N(C_2H_5)_2$	H	H, H	H, H	3.48	12
$\mathbf{A_3}$	$N(C_4H_9)_2$	H	H, H	H, H	3.44	12
$\mathbf{A_4}$	$N(iC_4H_9)_2$	H	H, H	H, H	3.46	12
$\mathbf{A_5}$	$N(C_2H_5)C_6H_5$	H	H, H	H, H	3.55	12
$\mathbf{A_6}$		H	H, H	H, H	3.21	12
$\mathbf{A_7}$	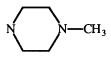	H	H, H	H, H	3.94	12
$\mathbf{A_8}$	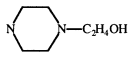	H	H, H	H, H	3.40	12
$\mathbf{A_9}$	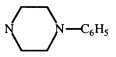	H	H, H	H, H	2.75	12
$\mathbf{A_{10}}$	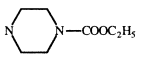	H	H, H	H, H	2.75	12
$\mathbf{A_{11}}$	NHC_2H_5	H	H, H	H, H	3.04	12
$\mathbf{A_{12}}$	$NHiC_4H_9$	H	H, H	H, H	3.11	12
$\mathbf{A_{13}}$	$NHCH_2C_6H_5$	H	H, H	H, H	3.12	12
$\mathbf{A_{14}}$	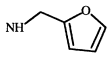	H	H, H	H, H	3.23	12
$\mathbf{A_{15}}$		H	H, H	H, H	3.01	12
$\mathbf{A_{16}}$		H	H, H	H, H	3.21	12
$\mathbf{A_{17}}$	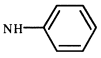	H	H, H	H, H	3.34	12
$\mathbf{A_{18}}$	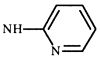	H	H, H	H, H	3.43	12
$\mathbf{A_{19}}$	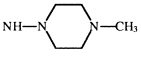	H	H, H	H, H	3.15	12
$\mathbf{A_{20}}$		H	H, H	H, H	5.44	13
$\mathbf{A_{21}}$		H	H, H	H, H	3.62	13
$\mathbf{A_{22}}$		H	(CH=CH)$_2$	H, H	4.82	13
$\mathbf{A_{23}}$	$N(CH_3)_2$	H	(CH=CH)$_2$	H, H	3.43	13
$\mathbf{A_{24}}$	$N(C_2H_5)_2$	H	(CH=CH)$_2$	H, H	4.11	13
$\mathbf{A_{25}}$	$N(C_4H_9)_2$	H	(CH=CH)$_2$	H, H	3.29	13
$\mathbf{A_{26}}$	$N(C_2H_4OH)_2$	H	(CH=CH)$_2$	H, H	3.30	13
$\mathbf{A_{27}}$		H	(CH=CH)$_2$	H, H	3.62	13
$\mathbf{A_{28}}$		H	(CH=CH)$_2$	H, H	4.12	13
$\mathbf{A_{29}}$	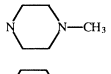	H	(CH=CH)$_2$	H, H	3.68	13
$\mathbf{A_{30}}$	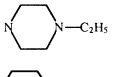	H	(CH=CH)$_2$	H, H	4.22	13
$\mathbf{A_{31}}$	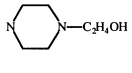	H	(CH=CH)$_2$	H, H	4.06	13

Table 4 (*continued*)

Compound	R^1	R^2	R^3, R^4	R^5, R^6	pIC_{50}[a]	Ref
A_{32}		H	H, H	$(CH=CH)_2$	4.67	13
A_{33}	$N(C_2H_5)_2$	H	H, H	$(CH=CH)_2$	3.05	13
A_{34}		H	H, H	$(CH=CH)_2$	3.92	13
A_{35}	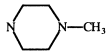	H	H, H	$(CH=CH)_2$	3.54	13
A_{36}	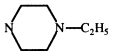	H	H, H	$(CH=CH)_2$	3.15	13
A_{37}	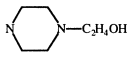	H	H, H	$(CH=CH)_2$	3.79	13
A_{38} (5r)	$NHCH_2CH_2NH_2$	H	H, H	H, H	2.75	(b)[b]
A_{39} (5q)	$NCH_3CH_2CH_2NHCH_3$	H	H, H	H, H	2.75	(b)
A_{40} (17b)	OCH_2CH_2OH	H	H, H	H, H	2.75	(b)
A_{41} (5n)	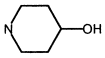	H	H, H	H, H	2.75	(b)
A_{42} (5o)	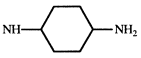	H	H, H	H, H	3.05	(b)
A_{43} (5e)		H	CH_3, H	H, H	4.73	(b)
A_{44} (5i)		H	CH_3, H	CH_3, H	4.83	(b)
A_{45} (5j)		H	H, Cl	H, H	4.68	(b)
A_{46} (17a)	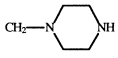	H	H, H	H, H	2.75	(b)
A_{47} (5b)		NO_2	H, H	H, H	3.10	(b)
A_{48} (5c)		CH_3	H, H	H, H	4.03	(b)
A_{49} (19c)		H	2H, 2H	2H, 2H	4.01	(b)
A_{50} (5d)		Br	H, H	H, H	3.64	(b)
A_{51} (5k)		H	H, H	H, H	3.79	(b)
A_{52} (5l)	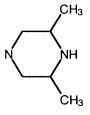	H	H, H	H, H	2.75	(b)
A_{53} (5p)		H	H, H	H, H	2.75	(b)
A_{54} (5h)		H	H, H	H, CH_3	4.03	(b)
A_{55} (5g)		H	H, H	CH_3, H	4.79	(b)
A_{56} (5f)		H	H, CH_3	H, H	4.73	(b)
A_{57}	$N(C_2H_5)_2$	C(=O)H	H, H	H, H	3.23	12
A_{58}	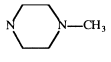	C(=O)H	H, H	H, H	3.23	12
A_{59} (5m)		H	H, H	H, H	3.25	(b)

[a]The IC_{50} values were determined in the assay with collagen 5.0 μg/mL.
[b]Described in the present paper.

Table 5. Chemical structures and platelet antiaggregating activity of compounds of class B

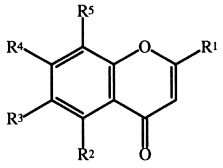

Compound	R^1	R^2, R^3	R^4, R^5	pIC_{50}[a]	Ref
B_1	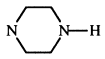	H, H	H, H	4.22	14
B_2	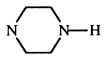	H, H	OC_2H_5, H	4.13	14
B_3	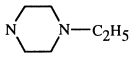	H, H	H, H	2.75	14
B_4	$HNCH_2CH_2NH_2$	H, H	H, H	3.19	14
B_5	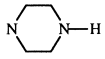	$(CH{=}CH)_2$	H, H	4.25	14
B_6	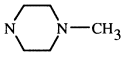	$(CH{=}CH)_2$	H, H	3.19	14
B_7	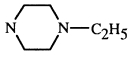	$(CH{=}CH)_2$	H, H	2.75	14
B_8		$(CH{=}CH)_2$	H, H	3.54	14
B_9	$N(C_2H_5)_2$	$(CH{=}CH)_2$	H, H	3.71	14
B_{10}	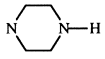	H, H	$(CH{=}CH)_2$	3.93	14
B_{11}	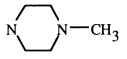	H, H	$(CH{=}CH)_2$	3.18	14
B_{12}	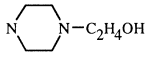	H, H	$(CH{=}CH)_2$	2.75	14
B_{13}	$N(C_2H_5)_2$	H, H	$(CH{=}CH)_2$	3.22	14

[a]The IC_{50} values were determined in the assay with collagen 10.0 μg/mL.

CoMFA relates the biological activities of a series of molecules with their steric and electrostatic fields calculated at several grid points around the molecule by means of a suitable probe, usually an sp^3 carbon atom with a charge of +1. Partial least squares (PLS[26]) is used as the regression method to develop the relationship between steric and electrostatic potentials and biological activity. The graphical representation of CoMFA model, in the form of coefficient isocontour maps, efficiently located the regions where the variation in steric and electrostatic properties of different molecules in a data set is correlated with the variation of biological activity. CoMFA isocontour maps may furnish useful indications to prioritize future synthesis and to develop sound working hypotheses on the nature of putative ligand–macromolecule interactions. Therefore, the main goal of our CoMFA study was the development of a three-dimensional model, able to interpret the changes in the antiplatelet activity, in terms of variations of steric and electrostatic characteristics of the analyzed compounds. Hopefully, such a model could suggest some structural modifications aimed at significantly improving the target activity of the examined compounds.

For the sake of clarity and an easier discussion of the results from the 3-D QSAR study, the analyzed compounds were grouped in six congeneric series—called A, B, C, D, E and F—and progressively numbered within each class (see Tables 4–9) (Chart 4).

In the first column of Tables 4–9, the diverse compound numbering used in the Chemistry section is also reported. Classes A–F comprised a quite diverse number of

Table 6. Chemical structures and platelet antiaggregating activity of compounds of class C

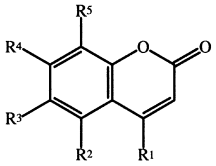

Compound	R^1	R^2, R^3	R^4, R^5	pIC_{50}[a]	Ref
C_1	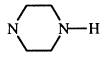	H, H	H, H	4.44	14
C_2	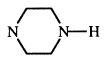	H, H	OC_2H_5, H	5.00	14
C_3	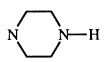	$(CH{=}CH)_2$	H, H	4.31	14
C_4	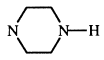	H, H	$(CH{=}CH)_2$	4.15	14

[a]The IC_{50} values were determined in the assay with collagen 10.0 μg/mL.

Table 7. Chemical structures and platelet antiaggregating activity of compounds of class D

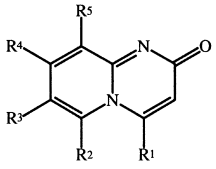

Compound	R^1	R^2, R^3	R^4, R^5	pIC_{50}[a]	Ref
D_1	$N(C_2H_5)_2$	$(CH{=}CH)_2$	H, H	3.41	13
D_2		$(CH{=}CH)_2$	H, H	3.26	13
D_3	$N(C_2H_5)_2$	H, H	$(CH{=}CH)_2$	3.44	13
D_4		H, H	$(CH{=}CH)_2$	3.42	13

[a]The IC_{50} values were determined in the assay with collagen 5.0 μg/mL.

compounds: 59 for class A (39 already reported and 20 described herein for the first time), 13 for class B, 4 for both class C and D, 3 for class E and finally only 1 for class F. The (3,5-dimethyl-1-piperazinyl) derivative $\mathbf{A}_{52}$ (**5l**), carrying a peculiar and unique structural variation at the piperazinyl ring, resulted a strong outlier and was not included in the CoMFA study.

The in vitro antiplatelet activity data shown in Tables 4–9 as pIC_{50} derive from the assay with collagen (5 μg/mL; 10 μg/mL for data from ref 14), since in this case a higher number of definite pIC_{50} could be obtained. However, in the case of $IC_{50} > 1000$ μM, a truncated pIC_{50} value of 2.75 was arbitrarily used to avoid the loss of relevant structural information for the modeling study.

Table 8. Chemical structures and platelet antiaggregating activity of compounds of class E

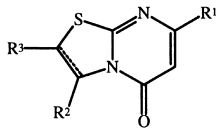

Compound	R^1	R^2	R^3	pIC_{50}[a]	Ref
E_1 (19b)	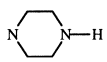	H	H	4.33	(b)
E_2 (20)	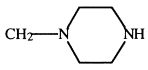	H	H	2.75	(b)
E_3 (19d)	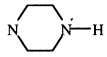	2H	2H	3.70	(b)

[a]The IC_{50} values were determined in the assay with collagen 5.0 μg/mL.
[b]Described in the present paper.

Table 9. Chemical structure and platelet antiaggregating activity of compound **19a** (class F)

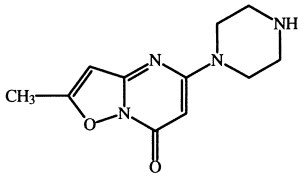

Compound	pIC_{50}[a]	Ref
F_1 (19a)	4.40	(b)

[a]The IC_{50} value was determined in the assay with collagen 5.0 μg/mL.
[b]Described in the present paper.

The pIC_{50} values of the 84 compounds tested for their in vitro antiplatelet activity cover a relatively wide range (from 2.75 to 5.44) and are acceptably well distributed along it.

The CoMFA study was performed within the QSAR module of SYBYL rel 6.4.[27]

In a first step the whole data set was divided in two parts, the *training set* (TS) and the *prediction set* (PS), composed by 73 and 10 molecules, respectively. The PS was chosen as to have representative molecules, with pIC_{50} values spanning in a regular way the full range of activities (see Table 11).

The molecular alignment chosen for the CoMFA study followed a conformational analysis on the amine substituents linked to the different rigid heterocyclic skeletons.

Most of the compounds bearing a cyclic amine presented a minimum energy conformer in which the amine and the heterocyclic planes were almost perpendicular.

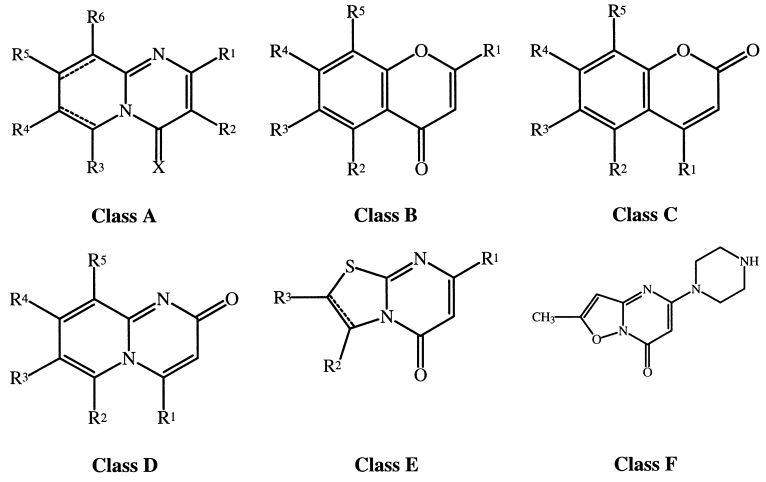

Chart 4.

On the other hand, compounds carrying secondary and tertiary amine substituents presented minimum energy conformers with the heterocyclic ring and the plane containing the three N–C bonds almost coplanar.

For the molecular overlay, the minimum energy conformer of the piperazinyl derivative **5a** was selected as the template because of its high activity and relatively low conformational freedom.

All the molecules in the TS were superimposed on the template **5a** by a pair-wise fit of the corresponding heavy atoms of the heterocyclic rings. To reach a better fit, the geometry of the minimum energy conformers was slightly modified by manual rotation around selected torsion angles of the amine substituents, allowing, occasionally, an energy penalty up to 5 kcal/mol.

The statistical parameters of the models derived for both neutral (N_1–N_{10}) and protonated (at the nitrogen of amine substituents) (P_1–P_6) molecules are listed in Table 10. For congeners with a further basic group on the amine substituents (i.e. $\mathbf{A_7}$, $\mathbf{A_8}$, $\mathbf{A_{20}}$ and $\mathbf{A_{22}}$) only the unconjugated nitrogen was considered protonated.

Unfortunately, the lack of parametrization of several fragments in structures A–F did not allow the calculation of molecular lipophilicity potential (MLP)[28] for 15 molecules, so that in the case of models based on neutral molecules (N_4–N_{10}) only 58 molecules remained in the TS; the situation was still worse when the protonated molecules were taken into account. As a consequence, no attempt to introduce the MLP as a third field was made.

A careful analysis of the statistical figures of the PLS models reported in Table 10 pointed out a similar fitting power for the two-field (steric plus electrostatic) models developed for neutral (N_1) and protonated (P_1) molecules. In terms of predictive ability, model P_1 is slightly better than model N_1, both showing improved statistics compared to single-field models (P_2, P_3 and N_2, N_3, respectively).

The examination of PLS models coming from the reduced set of 58 compounds revealed that the lipophilic field alone gave a very poor model (N_7) whereas statistically improved models were obtained with the two- and three-field combinations (N_8–N_{10}). These findings indicated that, besides the steric and electrostatic

Table 10. Statistical data of PLS models

Models	Fields	n	ONC	q^2	r^2	s
N_1	ste + ele	73	6	0.580	0.822	0.286
N_2	ste	73	6	0.508	0.764	0.330
N_3	ele	73	5	0.420	0.717	0.358
N_4	ste + ele	58	6	0.619	0.871	0.258
N_5	ste	58	6	0.474	0.799	0.323
N_6	ele	58	6	0.508	0.830	0.297
N_7	lipo	58	4	0.290	0.699	0.388
N_8	lipo + ste	58	4	0.603	0.794	0.321
N_9	lipo + ele	58	4	0.546	0.812	0.306
N_{10}	lipo + ste + ele	58	4	0.631	0.839	0.284
P_1	ste + ele	73	6	0.688	0.858	0.256
P_2	ste	73	6	0.495	0.751	0.339
P_3	ele	73	5	0.431	0.655	0.396
P_4	ste + ele	73	6	0.682	0.874	0.242
P_5	ste	73	5	0.392	0.723	0.357
P_6	ele	73	5	0.431	0.722	0.358

Table 11. Observed versus predicted platelet antiaggregating activity of compounds of the PS

Compound	pIC_{50} (obs)[a]	pIC_{50} (pred)[b]
$\mathbf{A_{38}}$	2.75	3.09
$\mathbf{A_{30}}$	4.22	3.66
$\mathbf{A_{24}}$	4.11	3.46
$\mathbf{A_{15}}$	3.01	3.24
$\mathbf{A_{50}}$	3.64	4.30
$\mathbf{A_7}$	3.94	3.48
$\mathbf{A_2}$	3.48	3.26
$\mathbf{A_{45}}$	4.68	4.47
$\mathbf{A_{33}}$	3.05	3.32
$\mathbf{A_{59}}$	3.25	3.65

[a]The IC_{50} values were determined in the assay with collagen 5.0 μg/mL.
[b]Predicted from model P_4.

properties, also the lipophilic characteristics of the tested compounds may play a role in the modulation of the antiplatelet activity.

The better statistics obtained for charged molecules (mod. P_1) prompted us to analyze for protonated compounds **8–13** also a different fitting criterion on the template **5a**. The two diverse fitting topologies explored (**a**) and (**b**) are reported in Chart 5.

Interestingly, the statistical figures of the two-field model developed from topology (**b**) (model P_4, Table 10) were comparable, or even slightly better in terms of fitting power, to those from topology (**a**) (model P_1). The good predictive ability of model P_4 can be appreciated by comparing the observed and predicted values reported in Table 11 for the PS.

Model P_4 was also selected to develop the coefficient isocontour maps reported in Figures 1 and 2. The steric isocontour map reported in Figure 1 showed sterically accessible regions (in green) occupied by 1-piperazinyl substituents of very active compounds and sterically hindered zones (in red) reached by substituents on piperazinyl nitrogen N_4 of molecules with low activity.

In the electrostatic isocontour map depicted in Figure 2, zones in which a high electron density favors or disfavors the biological activity are indicated by the magenta and white colors, respectively. Highly active molecules place their aromatic rings on the magenta zone, whereas low activity molecules occupy the white zone with electron-rich groups.

Conclusions

Considering the IC_{50} values obtained for the in vitro antiplatelet activity of compounds described here (Table 2), with reference to those afforded by 2-(1-piperazinyl)-4*H*-pyrido[1,2-*a*]pyrimidin-4-one **5a**[13] (Table 1), that is, the most active compound synthesized by us in this structural field, we can draw the following conclusions. (a) The presence of the 2-(1-piperazinyl) substituent as enamino group of the β-enaminonic moiety seems to be essential, or at least very favorable, to the activity of **5a**. (b) The introduction of properly chosen substituents in the free positions 6,7, and/or 8 (but not 3 and/or 9) of compound **5a**, as well as the replacement of the fused pyridine ring of **5a** with a suitable five- or six-membered heteroaromatic ring, can likely afford very active inhibitors of human platelet aggregation.

The 3-D QSAR study of the antiplatelet activity of more than eighty diverse compounds, structurally related to **5a**, gave further insight on the main physicochemical features governing the antiaggregating inhibitory properties in this chemical field.

In particular, both steric and electrostatic interactions seem to take place in well definite spatial locations, suggesting possible proper structural modifications for a significant improvement of the antiplatelet activity. An important influence of lipophilic interactions on the antiplatelet activity cannot be excluded. Unfortunately,

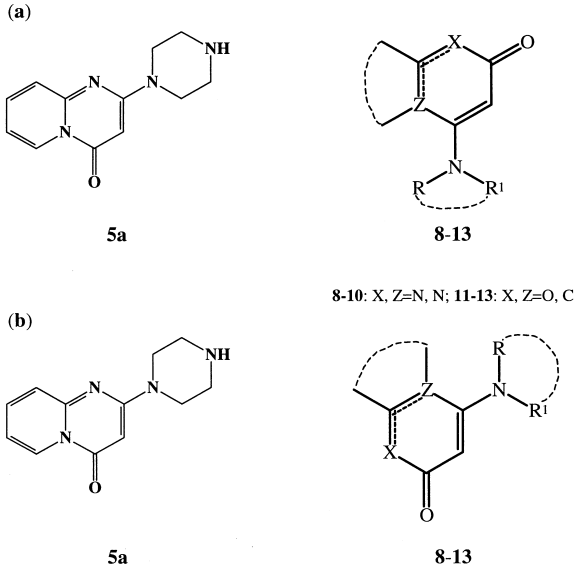

Chart 5.

Figure 1. Isocontour steric map for PLS model P_4 expressed as STDEV×COEFF. (contour levels: 0.039 *green*; −0.050 *red*. Color code: *green* increased activity, *red* decreased activity). Compounds $\mathbf{A_{20}}$, $\mathbf{A_{44}}$, $\mathbf{A_8}$ and $\mathbf{B_7}$ are shown to help interpretation.

Figure 2. Isocontour electrostatic maps for PLS model P_4 expressed as STDEV×COEFF. (contour levels: 0.042 white; −0.025 magenta. Color code: white decreased affinity for negative charge; magenta increased affinity for negative charge). Compounds $\mathbf{A_{31}}$, $\mathbf{A_{53}}$ and $\mathbf{C_2}$ are shown to help the interpretation.

the lack of parametrization of diverse fragments for the MLP calculations has not allowed the introduction of MLP as third field in our CoMFA study. The synthesis of new inhibitors carrying fully parametrized heteroaromatic fragments could help clarifying this important aspect of the structure–activity relationships.

Experimental

Chemistry

Melting points (mp) were determined using a Fisher–Johns apparatus and are uncorrected. IR spectra were recorded on a Perkin–Elmer 398 spectrophotometer (abbreviations relative to IR bands: br = broad, s = strong, w = weak, sh = shoulder). ^{1}H NMR spectra were recorded on a Hitachi Perkin–Elmer R 600 (60 MHz) spectrometer for compounds **5b–k,m,p**, **14b**, **15b,c,j**, **17a**, **19b–d**, **20** and on a Varian Gemini 200 (200 MHz) spectrometer for **5l,n,o,q,r**, **14a,c**, **15i**, **17b**, **18a**, **19a** and chemical shifts (δ) are reported in ppm using $(CH_3)_4Si$ as an internal reference (δ = 0). Spin multiplicities are given as follows: s (singlet), d (doublet), dd (double doublet), t (triplet), q (quartet), m (multiplet). Analyses of all new compounds were performed, for the indicated elements, by the Laboratorio di Microanalisi del Dipartimento di Scienze Farmaceutiche, University of Genoa, and the results were within ±0.4% of the theoretical values.

Thin-layer chromatograms were run on Merck silica gel 60 F_{254} precoated plastic sheets (layer thickness 0.2 mM). Column chromatography was performed using Carlo Erba silica gel (0.05–0.20 mM) or Carlo Erba neutral aluminium oxide (Brockmann activity I).

Ethyl 2-methyl-*N*-(2-pyridyl)malonamate (14a). Phosphorus pentachloride (17.39 g, 83.5 mmol) was slowly added to an ice-cooled stirred solution of ethyl hydrogen 2-methylmalonate (11.69 g, 80.0 mmol) in 80 mL of dichloromethane. The resulting solution was stirred at room temperature for 3 h, then 2-aminopyridine (4.99 g, 53.0 mmol), dissolved in 50 mL of dichloromethane and 40 mL of dry pyridine, was added dropwise so that the exothermic acylation of amine occurred. The mixture was further stirred at room temperature for 30 min, then poured into cold water (500 mL) and vigorously stirred overnight at room temperature. After careful addition of excess sodium carbonate with stirring, the organic layer was collected and the aqueous phase exhaustively extracted with dichloromethane. The combined extracts were washed with water, dried over anhydrous sodium sulfate, and solvents removed under reduced pressure. The resulting oil was distilled in vacuo and pure compound **14a** collected (6.01 g, 51%) as colorless thick oil, bp 114–115 °C (0.08 mM Hg). ^{1}H NMR ($CDCl_3$) δ 1.28 (t, 3H, CH_2CH_3), 1.51 (d, 3H, 2-CH_3), 3.48 (q, 1H, CH), 4.22 (q, 2H,CH_2CH_3), 7.06 (m, 1H, H-5′), 7.70 (m, 1H, H-4′), 8.18 (m, 1H, H-3′), 8.28 (m, 1H, H-6′), 9.20 (broad s, 1H, NH; disappeared with D_2O). IR (film) 3320 br (NH), 1745 (ester CO), 1700 (CO), 1602 w, 1583, 1530 br cm^{-1}. Anal. ($C_{11}H_{14}N_2O_3$) C, H, N.

Preparation of ethyl *N*-(5-chloro-2-pyridyl)malonamate (14b) and ethyl *N*-(5-methyl-3-isoxazolyl)malonamate (14c). The solution of 40.0 mmol of 5-chloropyridin-2-amine (5.10 g) or 5-methylisoxazol-3-amine (3.92 g) in 30 mL of dichloromethane and 10 mL of dry pyridine was added dropwise at room temperature to a stirred solution of ethyl 3-chloro-3-oxopropanoate (7.98 g, 53.0 mmol) in 30 mL of dichloromethane (an exothermic reaction with emission of white fumes occurred during the addition). The resulting warm mixture was stirred at room temperature for 30 min then poured into 300 mL of cold water; an excess of sodium carbonate was carefully added with stirring and the mixture was further stirred at room temperature for 1 h. The organic layer was then collected and the aqueous phase extracted several more times with dichloromethane. The combined extracts were washed with water, dried over anhydrous sodium sulfate, then evaporated to dryness in vacuo. By treating the nearly solid residue with a little ethyl ether, pure compound **14b** (8.64 g, 89%) or **14c** (5.52 g, 65%), respectively, separated out as a whitish solid which was then crystallized from the suitable solvent.

Compound 14b. Whitish solid, mp 109–110 °C (isopropyl ether). ^{1}H NMR ($CDCl_3$) δ 1.31 (t, 3H, CH_2CH_3), 3.57 (s, 2H, CH_2), 4.29 (q, 2H,CH_2CH_3), 7.71 (dd, 1H, H-4′), 8.09–8.46 (m, 2H, H-3′,6′), 9.80 (broad s, 1H, NH; disappeared with D_2O). IR ($CHCl_3$) 3410 and 3310 br (NH), 1728 (ester CO), 1698 (CO), 1594 w, 1579, 1522 br cm^{-1}. Anal. ($C_{10}H_{11}ClN_2O_3$) C, H, N, Cl.

Compound 14c. White crystals, mp 130.5–131 °C (ethyl acetate). ^{1}H NMR ($CDCl_3$) δ 1.31 (t, 3H, CH_2CH_3), 2.41 (s, 3H, 5′-CH_3), 3.49 (s, 2H, CH_2), 4.26 (q, 2H,CH_2CH_3), 6.67 (s, 1H, H-4′), 9.88 (broad s, 1H, NH; disappeared with D_2O). IR ($CHCl_3$) 3400 and 3280 br (NH), 1725 (ester CO), 1705 (CO), 1620, 1548 br cm^{-1}. Anal. ($C_9H_{12}N_2O_4$) C, H, N.

Preparation of chloroderivatives 15b,i and 18a. Following a procedure previously used[16] in the same chemical field, a mixture of 20.0 mmol of the appropriate compound **14**, 9.20 g (60.0 mmol) of phosphorus oxychloride and 1.50 g of polyphosphoric acid was heated with stirring at 130 °C for 3 h (110 °C for 1 h in the case of compound **18a**). After cooling, anhydrous ethanol (20 mL) was added and the mixture was further heated at reflux and stirred for 30 min, then allowed to cool. The chloroderivative was then recovered from the mixture as described below.

2-Chloro-3-methyl-4*H*-pyrido[1,2-*a*]pyrimidin-4-one (15b). The solution obtained from the reaction of **14a** (4.44 g) was poured into water (400 mL) and the whitish compound **15b** that separated out was collected by filtration, washed with water and dried (1.02 g, 26%); white crystals, mp 167–168 °C (ethyl acetate). ^{1}H NMR ($CDCl_3$) δ 2.35 (s, 3H, CH_3), 7.22 (m, 1H, H-7), 7.51–8.00 (m, 2H, H-8,9), 9.05 (m, 1H, H-6). IR ($CHCl_3$) 1668 br (CO), 1637, 1568, 1521 cm^{-1}. Anal. ($C_9H_7ClN_2O$) C, H, N, Cl.

2,7-Dichloro-4*H*-pyrido[1,2-*a*]pyrimidin-4-one (15i). From the reaction carried out with **14b** (4.85 g) a sus-

pension of yellowish crystalline solid was obtained. This solid was collected by filtration then treated with aqueous sodium carbonate, and the mixture was exhaustively extracted with dichloromethane. The combined extracts were washed with water and dried (anhydrous sodium sulfate). Removal of the solvent gave a solid residue from which, after treatment with a little ethyl acetate, pure compound **15i** was recovered (2.63 g, 61%); pale-yellow crystals, mp 222–222.5 °C (chloroform:ethanol 1:1). ^{1}H NMR ($CDCl_3$) δ 6.52 (s, 1H, H-3), 7.62 (d, $J_{9,8}$ = 9 Hz, 1H, H-9), 7.80 (dd, $J_{8,9}$ = 9 Hz, $J_{8,6}$ = 2.2 Hz, 1H, H-8), 9.07 (d, $J_{6,8}$ = 2.2 Hz, 1H, H-6). IR ($CHCl_3$) 1700 (CO), 1685 sh, 1630, 1558, 1509 cm^{-1}. Anal. ($C_8H_4Cl_2N_2O$) C, H, N, Cl.

5-Chloro-2-methyl-7*H*-isoxazolo[2,3-*a*]pyrimidin-7-one (18a). The reaction performed with 4.24 g of **14c** afforded a final suspension that was worked up exactly as described above for the corresponding suspension in the case of **15i**. Pure compound **18a** (1.26 g, 34 %) was so obtained; whitish solid, mp 214–215 °C (ethyl acetate). ^{1}H NMR ($CDCl_3$) δ 2.60 (s, 3H, CH_3), 6.34 and 6.35 (s + s, 2H, H-3 + H-6). IR ($CHCl_3$) 1710 sh, 1686 (CO), 1618, 1560, 1500 cm^{-1}. Anal. ($C_7H_5ClN_2O_2$) C, H, N, Cl.

3-Bromo-2-chloro-4*H*-pyrido[1,2-*a*]pyrimidin-4-one (15c). The solution of 0.39 mL (7.5 mmol) of bromine in 5 mL of dichloromethane was added dropwise at room temperature to a stirred solution of 0.90 g (5.0 mmol) of compound **15a**[17] in 10 mL of dry pyridine. The resulting mixture was stirred at room temperature for 15 min. The orange solid that separated out was collected by filtration then treated with 10% aq sodium carbonate, and the mixture was extracted several times with dichloromethane. The combined extracts were washed twice with 10% aq sodium carbonate then with water, and dried over anhyd sodium sulfate. After removal of solvents, the solid residue was taken up in a little ethyl ether and filtered to give 1.11 g (85%) of pure **15c**; whitish crystals, mp 224 °C (ethyl acetate with charcoal). ^{1}H NMR ($CDCl_3$) δ 7.30 (m, 1H, H-7), 7.53–8.03 (m, 2H, H-8,9), 9.08 (m, 1H, H-6). IR ($CHCl_3$) 1688 (CO), 1633, 1551 w, 1510 cm^{-1}. Anal. ($C_8H_4BrClN_2O$) C, H, N.

2-Chloro-4*H*-pyrido[1,2-*a*]pyrimidine-4-thione (15j). A mixture of 0.90 g (5.0 mmol) of compound **15a**,[17] 2.43 g (6.0 mmol) of Lawesson's reagent and 50 mL of anhydrous toluene was heated at reflux for 3 h, while stirring. The solvent was then removed under reduced pressure and the residue was taken up in a little dichloromethane and chromatographed on a neutral aluminium oxide column, eluting with the same solvent. The eluate collected, after removal of solvent, afforded pure compound **15j** as yellow crystals (0.79 g, 80%); mp 182–183 °C (ethyl acetate). ^{1}H NMR ($CDCl_3$) δ 7.30–8.26 (m, 3H, H-7,8,9), 7.74 (s, 1H, H-3), 10.29 (m, 1H, H-6). IR ($CHCl_3$) 1637, 1565 s, 1526, 1151 (CS) cm^{-1}. Anal. ($C_8H_5ClN_2S$) C, H, N, Cl, S.

3-Nitro-2-(1-piperazinyl)-4*H*-pyrido[1,2-*a*]pyrimidin-4-one (5b). A cold solution of 0.40 mL of 99% nitric acid in 2 mL of 96% sulfuric acid was added dropwise to a stirred ice-cooled suspension of compound **5a** (1.04 g, 4.5 mmol) in 20 mL of 96% sulfuric acid. The resulting yellow solution was stirred at 0 °C for 15 min, then poured onto crushed ice. The solution obtained was made alkaline by adding excess 28% aq ammonia solution, then exhaustively extracted with chloroform. The combined extracts were dried (anhyd sodium sulfate) and evaporated to dryness in vacuo to yield a yellow solid residue, which was taken up in a little ethyl ether and filtered to afford 0.86 g (69%) of pure **5b**; yellow crystals, mp 174–176 °C dec (ethyl acetate). ^{1}H NMR ($CDCl_3$) δ 1.78 (s, 1H, NH; disappeared with D_2O), 2.96 (m, 4H, CH_2NH), 3.65 (m, 4H, NCH_2), 7.01 (m, 1H, H-7), 7.32 (m, 1H, H-9), 7.79 (m, 1H, H-8), 8.90 (m, 1H, H-6). IR (KBr) 3312 w (NH), 1680 (CO), 1630, 1543 s,br, 1519 sh cm^{-1}. Anal. ($C_{12}H_{13}N_5O_3$) C, H, N.

General procedure for synthesis of substituted 2-amino-4*H*-pyrido[1,2-*a*]pyrimidin-4-ones 5c–j,l–r and 2-(1-piperazinyl)-4*H*-pyrido[1,2-*a*]pyrimidine-4-thione (5k). A mixture of the suitable amine (40.0 mmol) and 2-chloroderivative **15** (4.0 mmol), and 50 mL of ethanol was refluxed for 1–4 h, while stirring, then evaporated to dryness under reduced pressure. The residue obtained was partitioned between water and chloroform, and the aqueous phase extracted several more times with chloroform. The combined extracts (dried over anhyd sodium sulfate), after removal of solvents, afforded an oily or solid residue from which compound **5** was recovered as described below.

2-(1-Piperazinyl) substituted compounds 5c–k. The thick oily residues obtained from the reactions of piperazine with 2-chloroderivatives **15b**,**c**, **15d**,[16] **15e–g**,[29] **15h**,[16] **15i**, or **15j** were treated with a little ethyl acetate–ethyl ether. After standing, compounds **5c–k**, respectively, separated out as white or whitish solids (yellow solid in the case of thione **5k**) which were recovered by filtration, dried and crystallized from the suitable solvents.

Compounds 5l,n,o. The solid residues obtained from the reactions of **15a**[17] with 2,6-*cis*-dimethylpiperazine, 4-hydroxypiperidine, or 1,4-*trans*-diaminocyclohexane, were taken up in a little ethyl acetate and filtered; thus the pure compounds **5l**, **5n** or **5o**, respectively, were obtained as white solids which were then crystallized from the suitable solvents.

2-[(1-Piperidinyl)amino]-4*H*-pyrido[1,2-*a*]pyrimidin-4-one (5p). The thick oil obtained from the reaction of **15a**[17] with 1-aminopiperidine was chromatographed on a silica gel column, eluting with the mixture dichloromethane:ethyl acetate (1:1). The eluate collected, after removal of solvents, gave an oily residue which was treated with ethyl ether and allowed to stand so that pure compound **5p** separated out as a white solid which was then crystallized from isopropyl ether.

Compounds 5m,q,r. The thick oily residues derived from the reactions of **15a**[17] with homopiperazine, *N*,*N*′-dimethylethylenediamine, or ethylenediamine were dissolved in a little anhyd ethanol and treated with an ethanolic solution of maleic acid (0.50 g) (in the case of com-

pounds **5q,r** further addition of some ethyl ether and standing at 4 °C were then necessary). This way pure maleates of compounds **5m**, **5q** or **5r**, respectively, separated out as white crystalline solids which were recrystallized from the suitable solvents.

IR and ^{1}H NMR spectra of compounds **5m,q,r** were recorded using pure samples of the free amines, obtained from analytical samples of the corresponding maleates.

Data of compounds **5c–r** are reported in Table 3.

Preparation of 2-[(1-piperazinyl)methyl]-4*H*-pyrido[1,2-*a*]pyrimidin-4-one (17a) and 7-[(1-piperazinyl)methyl]-5*H*-thiazolo[3,2-*a*]pyrimidin-5-one (20). A mixture of 5.0 mmol of (chloromethyl)derivatives **16a**[20] (0.97 g) or **16b**[20] (1.00 g), 50.0 mmol (4.31 g) of piperazine and 80 mL of ethanol was refluxed for 30 min, while stirring. After removal of solvent in vacuo the residue was partitioned between water and chloroform, then the aqueous phase was extracted several more times with chloroform. The combined extracts (dried over anhyd sodium sulfate) were evaporated to dryness under reduced pressure to give an oily residue from which, after treatment with a little ethyl ether, compound **17a** (0.55 g, 45%) or **20** (0.60 g, 48%), respectively, separated out as a whitish solid.

Compound 17a. Whitish crystals, mp 139–140 °C, after crystallization from ethyl acetate–petroleum ether with charcoal. ^{1}H NMR ($CDCl_3$) δ 1.63 (s, 1H, NH; disappeared with D_2O), 2.55 (m, 4H, CH_2NH), 2.98 (m, 4H, NCH_2), 3.57 (s, 2H, 2-CH_2N), 6.73 (s, 1H, H-3), 6.99–7.43 (m, 1H, H-7), 7.55–7.90 (m, 2H, H-8,9), 9.10 (m, 1H, H-6). IR (KBr) 3325 (NH), 1683 sh, 1665 br (CO), 1624, 1560 w, 1525 cm^{-1}. Anal. ($C_{13}H_{16}N_4O$) C, H, N.

Compound 20. Ivory-white crystals, mp 157–159 °C, after crystallization from ethyl acetate–isopropyl ether. ^{1}H NMR ($CDCl_3$) δ 1.63 (s, 1H, NH; disappeared with D_2O), 2.51 (m, 4H, CH_2NH), 2.97 (m, 4H, NCH_2), 3.48 (s, 2H, 7-CH_2N), 6.52 (s, 1H, H-6), 7.10 (d, $J_{2,3}$ = 5 Hz, 1H, H-2), 8.04 (d, $J_{3,2}$ = 5 Hz, 1H, H-3). IR (KBr) 3295 w (NH), 1663 br (CO), 1636 sh, 1560 sh, 1544 cm^{-1}. Anal. ($C_{11}H_{14}N_4OS$) C, H, N, S.

2-(2-Hydroxyethoxy)-4*H*-pyrido[1,2-*a*]pyrimidin-4-one (17b). A mixture of **15a**[17] (0.90 g, 5.0 mmol), anhyd potassium carbonate (1.0 g) and ethylene glycol (15 mL) was heated with stirring at 160 °C for 1 h. After cooling, the mixture was poured into ice-water and the resulting solution was thoroughly extracted with dichloromethane. The combined extracts (dried over anhyd sodium sulfate), after removal of solvent, gave a solid residue which was taken up in ethyl ether and filtered. Pure compound **17b** (0.86 g, 83%) was so obtained; white crystals, mp 143–144 °C (ethyl acetate). ^{1}H NMR ($CDCl_3$) δ 3.15 (broad s, 1H, OH; disappeared with D_2O), 3.97 (m, 2H, OCH_2CH_2OH), 4.49 (m, 2H, OCH_2CH_2OH), 5.85 (s, 1H, H-3), 7.14 (m, 1H, H-7), 7.59 (m, 1H, H-9), 7.79 (m, 1H, H-8), 9.06 (m, 1H, H-6). IR ($CHCl_3$) 3360 br (OH), 1676 br (CO), 1636, 1568, 1518 cm^{-1}. Anal. ($C_{10}H_{10}N_2O_3$) C, H, N.

Preparation of (1-piperazinyl)derivatives 19a,b,d. A mixture of 4.0 mmol of the proper chloroderivative **18**, 3.44 g (40.0 mmol) of piperazine, and 50 mL of ethanol was refluxed for 1 h, while stirring. Following the procedure above described for the preparation of compounds **5c–k**, compounds **19a**, **19b** or **19d** were then obtained.

2-Methyl-5-(1-piperazinyl)-7*H*-isoxazolo[2,3-*a*]pyrimidin-7-one (19a). The reaction carried out with 0.74 g of **18a** yielded 0.41 g (42%) of **19a**·0.5 H_2O; whitish crystals, mp 146–147 °C (ethyl acetate). ^{1}H NMR ($CDCl_3$) δ 1.81 (s, 1H, NH; disappeared with D_2O), 2.49 (s, 3H, CH_3), 2.93 (m, 4H, CH_2NH), 3.54 (m, 4H, NCH_2), 5.33 (s, 1H, H-6), 6.08 (s, 1H, H-3). IR (KBr) 3390 br (OH), 3270 (NH), 1663 br (CO), 1621, 1583, 1527 br cm^{-1}. Anal. ($C_{11}H_{14}N_4O_2 \cdot 0.5H_2O$) C, H, N.

7-(1-Piperazinyl)-5*H*-thiazolo[3,2-*a*]pyrimidin-5-one (19b). Starting from 0.75 g of **18b**,[18] 0.75 g (79%) of **19b** was obtained; white crystals, mp 180–180.5 °C (ethyl acetate). ^{1}H NMR ($CDCl_3$) δ 1.81 (s, 1H, NH; disappeared with D_2O), 2.90 (m, 4H, CH_2NH), 3.60 (m, 4H, NCH_2), 5.36 (s, 1H, H-6), 6.74 (d, $J_{2,3}$ = 5 Hz, 1H, H-2), 7.85 (d, $J_{3,2}$ = 5 Hz, 1H, H-3). IR (KBr) 3275 (NH), 1650 br (CO), 1568 sh, 1552, 1513 cm^{-1}. Anal. ($C_{10}H_{12}N_4OS$) C, H, N, S.

2,3-Dihydro-7-(1-piperazinyl)-5*H*-thiazolo[3,2-*a*]pyrimidin-5-one (19d). Compound **18c**[19] (0.75 g) afforded 0.65 g (68%) of **19d**; white crystalline solid, mp 200.5–201.5 °C (ethyl acetate). ^{1}H NMR ($CDCl_3$) δ 1.87 (s, 1H, NH; disappeared with D_2O), 2.89 (m, 4H, CH_2NH), 3.20–3.70 (m, 6H, NCH_2 + 2-CH_2), 4.43 (t, 2H, 3-CH_2), 5.17 (s, 1H, H-6). IR (KBr) 3280 w (NH), 1653 br (CO), 1635 sh, 1580, 1527 cm^{-1}. Anal. ($C_{10}H_{14}N_4OS$) C, H, N, S.

6,7,8,9-Tetrahydro-2-(1-piperazinyl)-4*H*-pyrido[1,2-*a*]-pyrimidin-4-one (19c). A solution of **5a**[13] (1.15 g, 5.0 mmol) in 80 mL of ethanol, in the presence of 0.5 g of 5% palladium on activated charcoal, was subjected to hydrogenation under 30 psi hydrogen pressure using a Parr apparatus. The mixture was shaken at room temperature until the hydrogen absorption ceased (3 h). The catalyst was then removed by filtration and the solution obtained was evaporated to dryness under reduced pressure. The resulting colorless oil was treated with ethyl ether:isopropyl ether (1:1) to give 0.52 g (44%) of pure compound **19c** as white solid; mp 94.5–95.5 °C (ethyl ether). ^{1}H NMR ($CDCl_3$) δ 1.65–2.20 (m, 4H, 7-CH_2 + 8-CH_2), 1.82 (s, 1H, NH; disappeared with D_2O), 2.62–3.20 (m, 6H, CH_2NH + 9-CH_2), 3.52 (m, 4H, NCH_2), 3.90 (m, 2H, 6-CH_2), 5.39 (s, 1H, H-3). IR ($CHCl_3$) 1655 sh, 1640 s (CO), 1577, 1534 cm^{-1}. Anal. ($C_{12}H_{18}N_4O$) C,H,N.

Biology

Platelet aggregation. Human blood of healthy volunteers was added to a 130 mM trisodium citrate aqueous solution (volume ratio 9:1), then centrifuged at 100 *g* for

30 min to give platelet-rich plasma (PRP). Platelet aggregation, performed in an Aggrecoder PA-3210 aggregometer (A. Menarini, Florence, Italy), was measured following the Born's turbidimetric method[30] and quantified by the light transmission reached after 3 min. PRP (500 μL) was preincubated at 37 °C for 2 min with solvent (dimethylsulfoxide, 5 μL) or drug solution before the addition of the platelet aggregation agent. PRP aggregation was induced by 5.0 μM ADP (Sigma), collagen from bovine tendon (Mascia Brunelli) at the final concentration of 5.0 μg/mL, or 20.0 μM A 23187 (Sigma). Before each experiment the stock solutions of ADP (saline), collagen (saline), and A 23187 (DMSO) were diluted in saline.

Calculation of inhibition. In order to calculate the percentage of inhibition, the extent of aggregation measured in the presence of the compounds tested was always compared with that measured for a control sample containing the solvent, in an experiment carried out under the same conditions. From each series of experiments, in which the inhibitors were tested in at least five concentrations, a percentage inhibition–concentration curve was derived. From this curve the IC_{50} value was calculated as the concentration of inhibitor causing a 50% inhibition of the aggregation. The IC_{50} values reported in Table 2 are averages (± standard deviation) of those obtained from at least four different batches of platelets (usually 5–8 batches).

Molecular modeling and CoMFA

Molecular models of the neutral and protonated molecules were constructed with standard bond distances and angles using the molecular modeling software Sybyl version 6.4[27] running on a Silicon Graphics Indigo2 R4400 workstation.

The conformational analysis was carried out with the SYSTEMATIC SEARCH option of SYBYL, screening the conformational space of the selected torsion angles at 30° increments.

The geometries of all conformers generated in the conformational analysis were optimized by molecular mechanics (Tripos Force Field), and the conformers having an energy up 2 kcal/mol above the global minimum reoptimized by AM1 Hamiltonian using the parameter set reported in the MOPAC suite of programs.[31] The partial Mulliken atomic charges from AM1 calculations were used in the CoMFA study.

In CoMFA a three-dimensional cubic lattice, with a 2 Å grid spacing, was generated around the aligned compounds based on the molecular volume of the structures (grid beyond the molecules extended by 4.0 Å in all directions). Steric and electrostatic potentials were generated by a sp^3 carbon atom probe with a charge of +1. The option 'drop electrostatic' was set to NO.

The CoMFA models were derived by the partial least squares (PLS) method, implemented in Sybyl, with the leave-one-out cross validation procedure.[32]

The predictive ability of the model was measured as q^2 which is defined as:

$$q^2 = (\mathrm{SD} - \mathrm{PRESS})/\mathrm{SD}$$

where $\mathrm{PRESS} = \Sigma(\mathrm{Ypred} - \mathrm{Yactual})^2$ and $\mathrm{SD} = \Sigma(\mathrm{Yactual} - \mathrm{Ymean})^2$.

SD is the sum of squares of deviations of the observed values from their mean and PRESS is the prediction error sum of squares.

CoMFA was carried out on the TS in two subsequent steps. Firstly, starting with a number of latent variables equal to 8 and a number of cross-validation groups equal to the number of examined compounds, the optimal number of components (ONC) was determined. In the second step, the final models were developed by a conventional (non-crossvalidated) regression analysis with the ONC equal to that yielding the highest q^2 value.

Since the final equations are not very useful to represent efficiently the CoMFA models, three-dimensional graphics or isocontour maps were developed. They represent areas in the space where steric and electrostatic interactions are responsible for the observed variations of the biological activity. The graphical results from our final PLS model P_4 are represented in Figures 1 and 2.

Acknowledgements

The financial support from MURST (Rome), University of Genova and University of Bari is gratefully acknowledged.

References and Notes

1. Ermili, A.; Mazzei, M.; Roma, G.; Cacciatore, C. *Il Farmaco-Ed. Sci.* **1977**, *32*, 375.
2. Ermili, A.; Balbi, A.; Di Braccio, M.; Roma, G. *Il Farmaco-Ed. Sci.* **1977**, *32*, 713.
3. Ermili, A.; Roma, G. *Gazz. Chim. Ital.* **1971**, *101*, 269.
4. Ermili, A.; Roma, G.; Balbi, A. *Gazz. Chim. Ital.* **1971**, *101*, 651.
5. Ermili, A.; Balbi, A.; Roma, G.; Ambrosini, A.; Passerini, N. *Il Farmaco-Ed. Sci.* **1976**, *31*, 627.
6. Roma, G.; Vigevani, E.; Mazzei, M.; Ermili, A.; Ambrosini, A.; Passerini, N. *Il Farmaco-Ed. Sci.* **1978**, *33*, 822.
7. Mazzei, M.; Balbi, A.; Roma, G.; Di Braccio, M.; Leoncini, G.; Buzzi, E.; Maresca, M. *Eur. J. Med. Chem.* **1988**, *23*, 237.
8. Mazzei, M.; Sottofattori, E.; Di Braccio, M.; Balbi, A.; Leoncini, G.; Buzzi, E.; Maresca, M. *Eur. J. Med. Chem.* **1990**, *25*, 617.
9. Leoncini, G.; Maresca, M.; Colao, C.; Buzzi, E.; Mazzei, M.; Balbi, A. *Pharmacol. Res.* **1991**, *23*, 139.
10. Leoncini, G.; Maresca, M.; Colao, C.; Buzzi, E.; Mazzei, M. *Cell. Biochem. Funct.* **1991**, *9*, 79.
11. Hermecz, I.; Meszaros, Z. In *Advances in Heterocyclic Chemistry*; Katritzky, A. R., Ed.; Academic: New York, 1983; Vol. 33, pp 241–330.

12. Roma, G.; Di Braccio, M.; Leoncini, G.; Aprile, B. *Il Farmaco* **1993**, *48*, 1225.
13. Di Braccio, M.; Roma, G.; Leoncini, G. *Eur. J. Med. Chem.* **1995**, *30*, 27.
14. Di Braccio, M.; Roma, G.; Leoncini, G.; Poggi, M. *Il Farmaco* **1995**, *50*, 703.
15. Leoncini, G.; Signorello, M. G.; Roma, G.; Di Braccio, M. *Biochem. Pharmacol.* **1997**, *53*, 1667.
16. Hermecz, I.; Horvoth, A.; Vasvári-Debreczy, L.; Meszaros, Z. *Synthesis* **1984**, 152
17. Snyder, H. R.; Robison, M. M. *J. Am. Chem. Soc.* **1952**, *74*, 4910.
18. Di Braccio, M.; Roma, G.; Mazzei, M.; Balbi, A.; Testa, R. *Il Farmaco-Ed. Sci.* **1986**, *41*, 183.
19. Glennon, R. A.; Bass, R. G.; Schubert, E. *J. Heterocyclic Chem.* **1979**, *16*, 903.
20. B'hme, H.; Weisel, K. H. *Arch. Pharm.* **1977**, *310*, 26.
21. Roma, G.; Ermili, A.; Di Braccio, M.; Mazzei, M. *Il Farmaco-Ed. Sci.* **1982**, *37*, 747.
22. Roma, G.; Di Braccio, M.; Balbi, A.; Mazzei, M.; Ermili, A. *J. Heterocyclic Chem.* **1987**, *24*, 329.
23. Di Braccio, M.; Roma, G.; Mazzei, M.; Balbi, A.; Schiantarelli, P.; Cadel, S.; Bongrani, S. *Il Farmaco-Ed. Sci.* **1988**, *43*, 705.
24. Di Braccio, M.; Roma, G.; Grossi, G. C.; Ciarallo, G. *J. Heterocyclic Chem.* **1992**, *29*, 25.
25. Cramer, R. D.; Patterson, D. E.; Bunce, J. D. *J. Am. Chem. Soc.* **1988**, *110*, 5959.
26. Dunn, Jr III, W. J.; Wold, S.; Edlund, U.; Helberg, S. *Quant. Struct.-Act. Relat.* **1994**, *3*, 131.
27. Sybyl: *Molecular Modelling Package*; Tripos Ass., St Louis, MO, USA.
28. Gaillard, P.; Carrupt, P.-A.; Testa, B.; Boundon, A. *J. Comput-Aided Mol. Design* **1994**, *8*, 83.
29. Ingalls, E. A.; Popp, F. D. *J. Heterocyclic Chem.* **1967**, *4*, 523.
30. Born, G. V. R. *Nature (London)* **1962**, *194*, 927.
31. AM1 quantomechanical semiempirical method can be found on the package MOPAC 6.0 which is available from QCPE (506).
32. Cramer, Jr III, R. D.; Bunce, J. D.; Patterson, D. E. *Quant. Struct.-Act. Relat.* **1988**, *7*, 18.